A computer based model for lung cancer analysis

Fatma Ayari[1], Mekki Ksouri [2], Ali Alouani [3]

**[1,2] University of Tunis Elmanar, Electrical Engineering Department,
National School of Engineers Tunis (ENIT), B.P.342, Le Belvedere, 1002 Tunis, Tunisia**

**[3] Tennessee Technological University Electrical Engineering Department,
Po Box 5004, Cookeville, TN 38 505, USA,**

Abstract

In this paper, we have presented an innovative methodology to convey connection between physical and mechanical properties of lung tissue in some lung cancer diseases. It is proposed in this method to combine computed tomography (CT) medical images, image processing and Finite Element (FE) technique to grasp the patient lung tissue response under gradual stages of lung cancer. Finite Element models based on lung CT images of different patients are used to analyse the real behaviour of lung tissue and detect the difference between mechanical parameters in both normal and pathologic cases. Results show that normal lungs display distinct superiority in strength, and expansion properties. It is also notable that we have present new mechanical parameters to clearly describe the evolution of different patient's lung cancers cases. Investigating lung cancer using such techniques is very promising to enhances data monitoring towards the development of automated diagnosis systems.

Keywords: *Computed Tomography, Lung cancer, Image processing, Finite Element Analysis.*

1. Introduction

In biomechanical simulation, finite element method (FEM) has been considered to be one of the best tools for modeling objects with complex geometry, various materials, complex loading paths and boundary conditions, such as the human tissues [1-10]. In previous studies dealing with FEM in biomechanical simulation 3D models have been mostly involved. These models are sometimes complicated, time consuming and do not converge obviously with realistic behavior of biologic organs behavior. We are presenting here a new numerical 2D FEM based model on the basis of actual CT biomedical images to investigate the correlation between stresses developed in the biomechanical lung tissue at the vicinity of infected tissue and various steps evolution of lung cancer disease. This study was conducted based on data from patients with different gender and age, who are presenting the same lung pathology. In fact, we are interested with lung cancer because it is responsible in most deaths for both men and women; it is the most deadly form of cancer death. Smoking, exposure to passive smoking and practice of certain professional activities inside contaminated environments with radon, uranium, arsenic, nickel, chromium, tars etc, are known to be at the origin of most lung cancer diseases.

In this article we are dealing with a new FEM based methodology to predict the evolution of pulmonary lung disease, in the particular lung cancer pathology. In this approach the medical CT images with conjunction with image data processing have been used as a strong support to build the FEM model and to create correlation rule between FEM issued results and the evolution stages of the lung cancer disease. This study can be very useful in the medical applications to make a rapid predictive pathway tool of some diseases evolution.

Medical images of lung cancer have been loaded using Matlab software, where the boundaries of special parts have been marked using adequate image filtering and markers. Abaqus commercial code has been used to assemble the different organs presented in the CT images as parts which are prepared previously and then, imported using CATIA software. Imported parts simulating organs have been embedded into the whole model and quadrilateral reduced integration elements have been used to mesh the different parts. Material properties have been obtained from data in the literature [9-10]. Thus, in this investigation, simulations are used to analyze the Von Mises effective stress distribution, strains and the maximum principal stresses in the various lung regions. Moreover, the overall stresses and strains in the different tissues are calculated. We have conclude after comparison between different simulations that in overall examined cases, a concentrated relative high stress level is noticed at the vicinity of lung cancerous tissues. Nevertheless, it is also remarked a correlation between the evolution size of the lung cancerous tissue and the effective stress in the lung tissue. Description of the different steps toward final results and details of calculation are described in the following sections.

2. Interest of this work for the medical imaging

CT images can produce a huge amount of data, a typical CT dataset that is used for pulmonary embolism diagnosis can have more that 500 slices, the size of the smallest visible volume being in the order of magnitude of one millimeter. Computer aid can provide main goal by

decreasing the time required to perform an exam, and acting also as a safety measure for radiologists. In this work we are proposing a complementary tool to enhance the expertise of radiologist and to contribute to the development of automated diagnosis systems.

Cancers that develop in the lung may arise from a bronchial cell that has been developed: those lung cancers are then classified as primitive lung cancers. They are also classified into two subfamilies of primitive lung cancers: according to their cells size, they have different clinical presentation and radiological treatment. Small cell cancers represent 15% of lung cancers they are called 'SC (small cells)' and non-small cell cancers that are now 85% of cases identified by 'NSC'. In other cases, lung cancer can be a metastasis of a primary cancer developed previously in another organ; the lung indeed constitutes the first target organ for metastasis. In this work we are interested with lung cancer due to metastasis of primary cancer. In essence, the method should be able to tell where potential regions of risk exist in the medical image, where lung cancerous tissues are highly probable, and that the physician can in order carefully validate the presence or absence of lung cancer.

3. Image processing methodology

The principle image processing work in this paper takes the form of framework, where CT images of lung cancer from different patients are collected, segmentation of thorax organs was computed, then, lung cancerous tissues were detected and then the detection results are evaluated against the same detection process made by a radiologist.
Segmentation of lung cancer images is a challenging task by itself, because of the particular shapes of thorax complexity of organs, which are stretched out and multi-scale structures. The main difficulty of lung cancer images segmentation is that the lung cancerous tissue is surrounded by other tissues, and it shares sometimes a lot of characteristics with other organs tissues. For these reasons, we have tested various techniques used in image segmentation processing, then we have choose a novel application based on active contour method which is based on the energy criterion. In this segmentation technique different algorithms can be used, the Caselles algorithm [10], have been selected in this work because it has allowed the best convergence for the overall CT image presented in this study. This method works by growing a wave front from an initial simple shape that is set inside the lung cancer by a radiologist, and the interest of this application is in the way this wave is guided by advanced information, that is, the priori knowledge of the non lung cancerous organs shape [11], this method is build based on energy criterion. The used algorithm is a contour-based method i.e. the gradient of the image is used to compute the force function. The curve will thus be driven to regions with high gradient.
This method does not require any regularization term as it is intrinsic to the method. It is implemented as a signed distance function and is reinitialized every iteration. The specific parameter of this algorithm is the number of iterations that can be tuned all depends on the surface of the contour.
Contour detection technique of the lung cancer tissue used in this survey found the majority of contours with a good accuracy. We are giving now some examples from medical lung cancer data sets considered in this work, using CT images. The scan images are collected from Salah Azaiez National Cancer Institute of Tunisia database. Patients have body mass index (BMI) between 25 and 40. Figure 1 gives a scheme of the prospects that permits not only a quantitative but also a visual assessment of the method, illustrating the detection contour of the affected cells. Figures 2 to 7 prove the different steps of detecting contours for different cases. Some measures are being possible using Matlab programs and they have been used to build sketches of different models.

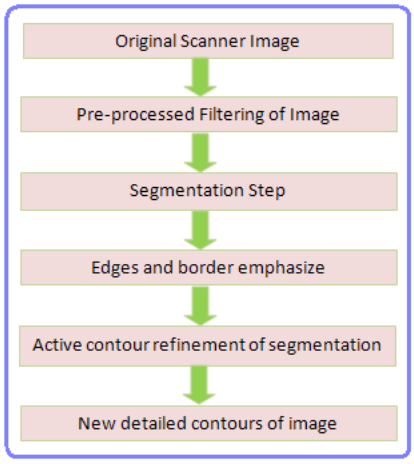

Fig 1 Prospects scheme for a more precise reconstruction: refinement of the segmentation by active contours

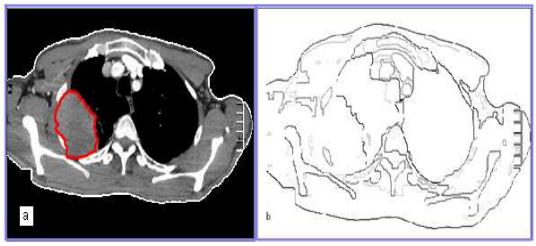

Fig 2 (a) CT image of patient (P_1) with Caselle segmentation algorithm [10] to highlight cancerous tissues, (b) edges and borders of the original plot of this patient.

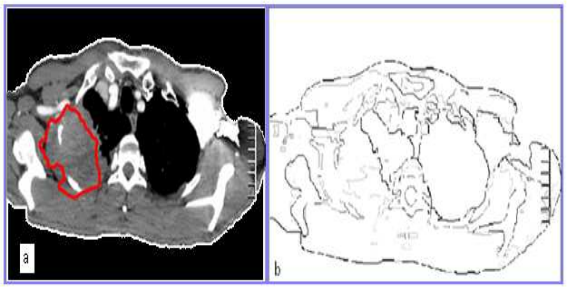

Fig 2 (a) CT image of patient (P_1) with Caselle segmentation algorithm [10] to highlight cancerous tissues at advanced stage, (b) edges and borders of the original plot for the patient.

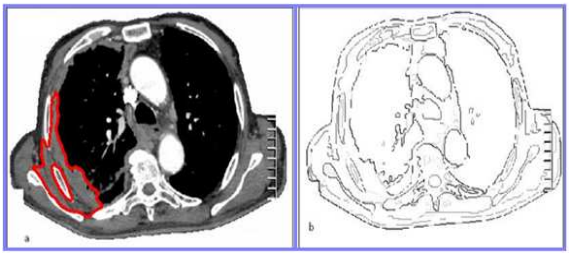

Fig 3 (a) CT image of patient (P_2) with Caselle segmentation algorithm [10] to highlight cancerous tissues, (b) edges and borders of the original plot.

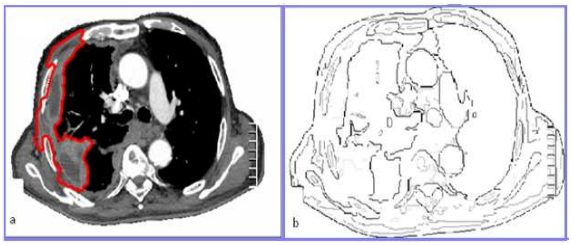

Fig 4 (a) CT image of patient (P_2) with Caselle segmentation algorithm [10] to highlight cancerous tissue, at advanced stage with development and presence of a tumour mass with invasion of bone. (b) Edges and borders of the original plot of the patient.

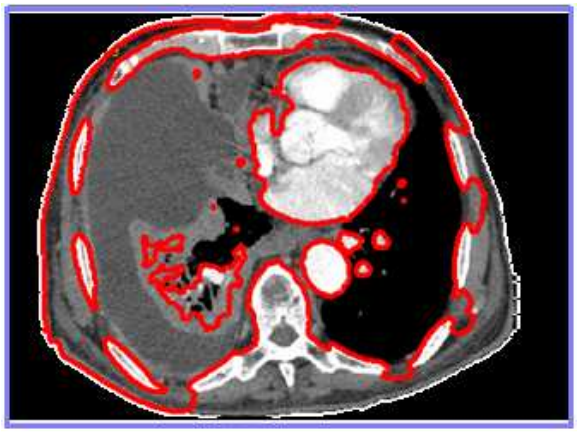

Fig 5 CT of patient (P_2) with Caselle segmentation algorithm [10] to highlight cancerous tissues, at advanced stage. Pleural effusion associated with nodular lymphadenitis. The figure shows the contour of the pleural effusion with red colour.

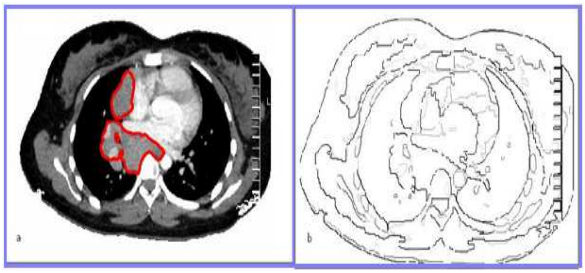

Fig 6 (a) CT image of patient (P_3) with Caselle segmentation algorithm [10] to highlight cancerous tissue. It is noticeable the presence of highly developed lymphadenopathy. (b) Edges and borders of the original CT image plot of this patient.

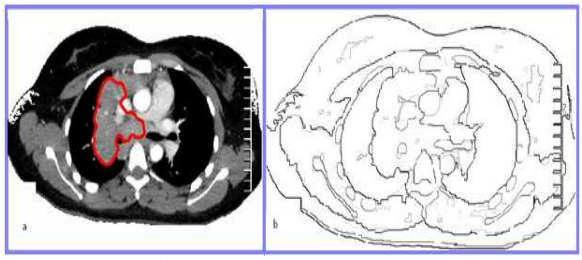

Fig 7 (a) CT image of patient (P_3) with Caselle segmentation algorithm [10] to highlight cancerous tissue after one month from the initial saved stage. It is noticeable the presence of highly developed lymphadenopathy. (b) Edges and borders of the original CT image plot of a patient.

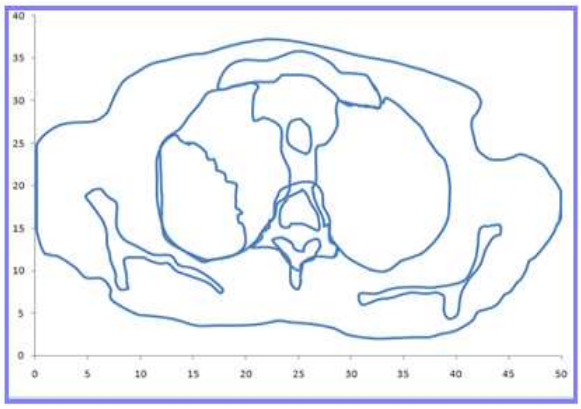

Fig 8 Sketch of the 2D CT image reproduction ttransforming pixels to data matrix before sketching.

The different images presented in this section have illustrated a high accuracy of the algorithm used to detect cancerous lung tissues at different stages. These results were very encouraging but they can be with a high usefulness if they can be merged into a technique that allow quantitative measurements of the different transformations associated to the progressive development of cancerous tissues. Thus, this information can be highly valuable for lung cancer diagnoses and also post treatment. Therefore, we have build different FEM models based on transformed CT images to 2D sketches reproducing the real shape of different organs and tissues with a high accuracy. A linear reduction scale was used to be with accuracy with real dimensions of the different organs. The following section details the different steps of FEM modelling and how we have take advantage within those models to promote lung cancer pathology.

4. Computational Finite Element modeling

In order to study the real mechanical properties of the pulmonary behaviour and distinguished the difference between different stages when lung cancerous tissue is being developed. A 2D model is established based on the anatomy of principle organs drown by the CT medical image. The FE model was generated from a CT-image set by interactively identifying different tissue groups using data image processing described via section.2. Regions of interest were identified by appropriate masks and provided into a 2D representation as it shown by Figure 8.
Image-based modelling is prepared then via IGS-format parts using CATIA software from images of different organ parts, and then imported to Abaqus FE package [12] to build the entire assembly of an overall FE model. CT Images are captured at 5 cm H_2O internal pressures showing tissue regions including the smooth muscles and the cartilage profiles as shown by Figure 2 to Figure 7.
Necessary dimensions of different organs are interpolated through a sketch deduced from CT images after application of contour filtering and data measurements within specific algorithms. Figure 16 shows the scheme toward transforming the original CT image of one patient to a finite element model (FEM), where plane stress hypothesis is adopted. Due to the complex anatomical structure of some external edges, some simplifying assumptions were mandatory. Essentially, the model was considered as composed of a cartilaginous zone, a smooth muscle zone for lung muscles and smooth connective tissue accounting for all the tissues covering the cartilage, inner and outer surfaces. The FE conceived models have been build from 10 patients' experimental CT images. They were collected for two cancer configurations stages, primary stage and advanced one. The patients were classified into male or female gender, age, weight and BMI factor as it is shown by the Table 1.

Table 1

Patient	Gender*	Age	Weight (kg)	BMI
Ideal	M	50	85	29
1	M	60	88	30
2	M	70	75	28
3	M	72	70	29
4	M	46	90	30
5	M	60	87	24
6	W	42	80	30
7	W	50	68	35
8	W	60	70	40
9	W	63	75	35
10	W	58	67	30

*M = men, W= women

4.1 Boundary conditions

Boundary conditions were defined at the highlighted surfaces Figure (10) and Figure (11): symmetry constraint along x direction at surfaces S_1 and S_2; symmetry constraint along y direction at surface S_3. Nodal displacement in the y and x directions is attributed to internal edges (red edge in figure (10)) to simulate the deformation of the tissue under the internal pressure that is varying from case to case and that is meticulously depending on the patient and his healthy state. Typical boundary conditions are replicated for all FE models. Loading parameter described above, will be discussed in further details in the following section. Connection between organs is ensured using multipoint constraints (MPC) between nodal regions embedded from an organ to another. Some external nodes have been fixed to ensure the stability of the model during loading.

Loads were assigned to simulate realistic conditions at various internal lung pressures applied through successive steps. A first step has been used to simulates internal normal pressure by attributing nodal displacements in the x and y direction, at external free lung surfaces. The following load steps simulate uniform pressure loads with a parametric pressure value that is varying in the range [5 to 40 cmH_2O], applied at the inner lung surfaces. This parameter will be also used further to deduce the behaviour of different tissues when simulating the evolution aspect of lung cancer. In fact, the measurement of the total-respiratory-system Pressure-Volume, has been well analysed in reference [13]. Pressure-Volume evolution, in normal and pathologic cases has been well discussed in this reference and it was demonstrated that there is a relation between internal lung pressure and the lung disease. This study has been motivating to focus on studying the effect of the lung internal pressure on the mechanical behaviour of the different organs, for all the analyzed cancerous cases.

After each loading step, the deformed configurations and the stress distribution in the specific tissues were extracted, Figure 10 (a) shows the limit of the free edge in the lung cancerous tissue highlighted in red, where pressure is applied. This red edge is only associated to internal pressure without any other reaction conducted by contact with other tissues. Figure 11 (b) is showing a red highlighted path that is selected for detecting stresses variation along this path. In fact we have designated such particular path to extract and represent stresses evolution in this region because this path is crossing both uncontaminated lung tissues and contaminated lung tissues. Stresses distribution due to internal pressure variation along this red path can bring information about the strength of the lung tissue in both normal and pathologic cases and also distinguishes between different pathologic cases.

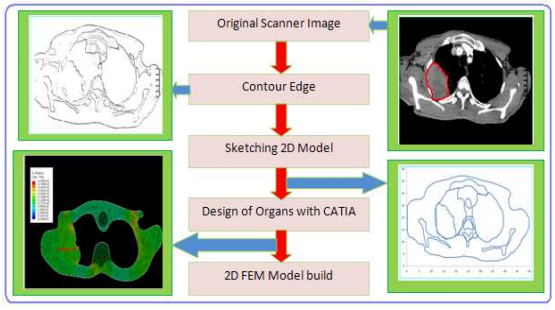

Fig 9 Prospects scheme steps toward the 2D FEM biomedical model from CT images.

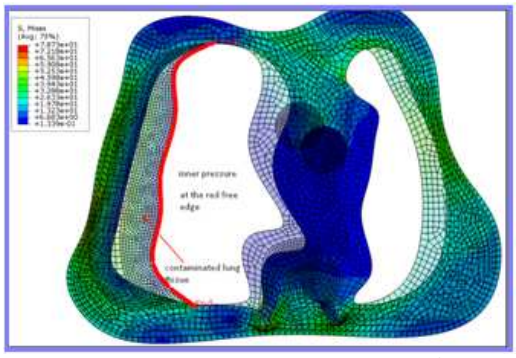

Fig 10 (a) boundary conditions; (internal pressure on the free red edge of lung tissue) case of patient P_4 at initial stage.

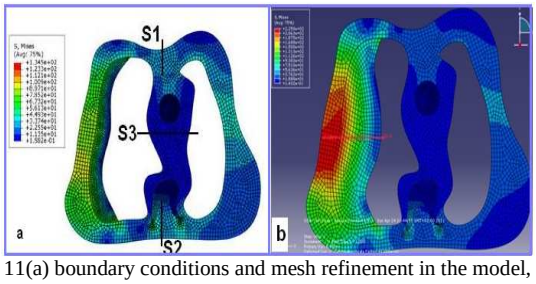

Fig 11(a) boundary conditions and mesh refinement in the model, (b) extractions of mechanical parameters along the red path

4.2 Tissues mechanical properties

Concerning the mechanical properties of pulmonary tissues for the different patients, the parameters related to the materials behaviour were set as based on studies carried out in literature review. In fact, both the cartilage and soft tissues were assumed to be homogeneous and isotropic materials. Soft tissues are assumed as non-linear, elastic and nearly incompressible materials. The various mechanical parameters are resumed in the Table 2 as it is mentioned in the reference [14].

Table 2

Model component	Element type	Density ρ Kg/m3	Young modulus E MPa	Poisons ratio ν
Skin	shell	1000	1.0	0.45
Vertebra discs	shell		17000	0.3
Ribs	shell	1000	17000	0.3
Lungs	shell	1000	2.02	0.475
Surrounding tissues	shell	1000	10	0.45

5. Analyses and discussion

Deformed configurations of the different simulated cancerous lungs show that lung responses are strongly dependent on the volume of the cancerous lung tissue and its shape. Figure 12 (a) and Figure 12 (b) are associated to the patient (P_5 in table 1) for both initial and advanced cancerous stages. Figure 13 is representing the pressure evolution along the loading path described above, for both primitive and advanced cancer lung pathology corresponding to patient (P_5). These two figures have well emphasized the pressure evolution in the described path, for both primary and advanced stages. It is well established a rapid increase in the pressure values in cancerous tissues. Thus, in the case of advances cancerous stage, the pressure is higher in overall tissues and also the slope of the trend pressure curves is mostly higher then initial case. This fact can be associated to the rigidity increasing in the pulmonary cancerous tissue that is acquired as an additional amount of mass tissue is significantly occurring. Also, the drop of pressure is due to wider internal contact surface between both soft and contaminated lung tissue, which is due to the larger mass of cancerous tissue. In turn, when the internal pressure load is increasing, the overall stresses are increasing also in the same way. Indeed, it is well shown that the stress amplitude is also increasing almost in the same way as pressure. According to the model presented by figure 14, and simulating earliest cancerous stage of patient P_6, it is remarked that at the vicinity of the contaminated tissue the gradient of stresses is being changed. Thus, the downfall of stress curves for various pressure values is characterized with a law rate. A small concentrated stress field appears in many parts of the model, in particular at the vicinity of abrupt changes in the lung tissue shape. Figure 15 is representing stresses along the normal path (highlighted in red) from the FE model illustrated by Figure 14, it shows similar downfall behavior for all internal pressure values. A stress representation for the advanced cancer stage of patient P_6 is also exemplified by Figure 16. We can conclude that, the existence of cancerous lung tissue reduces the mechanical resistance of the lung. But this collapse is depending on the amount of contaminated lung tissue and the mass distribution in the lung.

The stress-distance curves are plotted for every one of the simulated cases. The maximum principal stresses in the lung tissue for various patients are simulated at the earliest cancerous stage and advanced one, with internal pressure of 5 cm H_2O. Those values are variable and they are meticulously depending on the contaminated lung surface or volume, the cancerous mass concentration, the gender and the BMI of patients and so on. If we decide to take advantage from the simulation investigation, we have to consider new independent variables that can bring correlated information indicating the severity of the disease and to compare between patients state evolution. This could put in light the behavior of cancer lung disease and then enhance therapeutic medicine. Hence, it is noticed that only the ribs and muscle display appreciable values for mechanical stresses; the stresses in the connective tissues are almost negligible, that is due to the fact that these tissues are assumed to be large deformable materials.

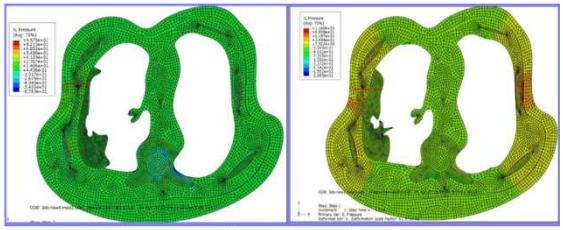

Fig 12 stresses along the different parts of the model, patient P_5 at earliest cancerous stage (a) and (b) at cancerous advanced stage.

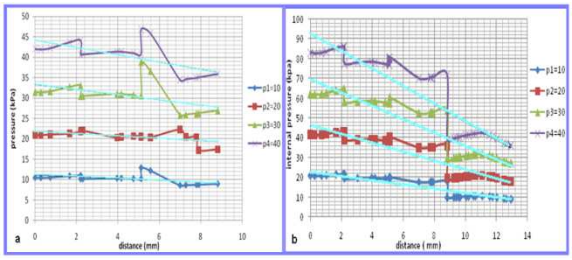

Fig 13 stresses vs distance for the different pressure values, patient P_5, at earliest cancerous stage (a), and advanced cancerous stage (b).

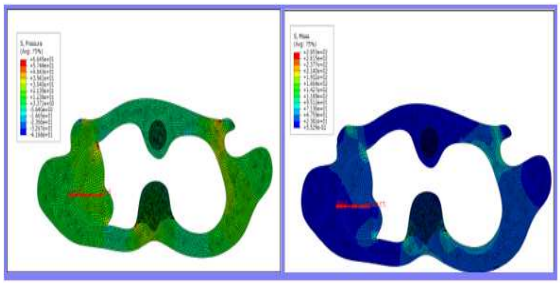

Fig 14 (a) pressure plotted along the different tissues, (b) Mises stresses along the different parts of the model patient P_6.

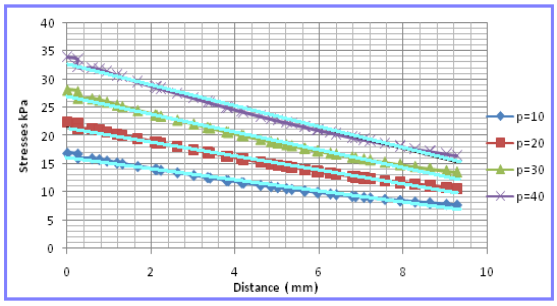

Fig 15: Stresses vs distance for the different pressure values. (Patient P_6 at earliest stage)

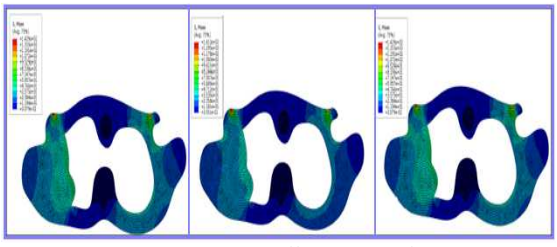

Fige 16: Stress evolution during different steps of pressure loading, evolution of stresses distribution according to pressure values (patient P_6)

5.1 First FE parametric analyses

The quasi-static pressure-volume P-V relationship is one aspect of lung mechanical behavior that was used in many researches to obtain information about how lungs deform during breathing in health and disease. Moreover, the PV curves have been widely studied in various pathological cases but adapted especially for intense respiratory trauma distress. Several theoretical and experimental works have attempted to explain the nature of the pressure volume curves P-V when breathing is forced [13-17]. But, access to the real interaction between the lung and the chest wall and other organs under the effect of pressure change was always difficult and it is still poorly mastered by clinicians and experimentalists. We have attempted to explain the relation between pressure and volume variation in the case of cancerous lungs, based on a simulation approach that takes into account interaction between the different thoracic organs.

So far, to study the evolution of remarkable characteristics of lung cancer at various stages accordingly to different internal pressures values, we have investigated in this first parametric numerical study, the evolution of lung volume firstly, and the BMI parameter secondly. As far as we are dealing with 2D CT images, we have introduced the concept of unit volume fraction within the hypothesis that this volume corresponds to surface per unit length. Two volume fractions are introduced via two parameters denoted; Vfds (volume fraction of deformed shape) and Vfads (volume fraction of advanced deformed shape). These two ratios are defined respectively; as follows:

First, the Vfds ratio refer to the ratio of lung tissue characteristic surface, contaminated with carcinogenic cells, divided by the lung surface characterizing the initial lung state.

Vfds = final deformed contaminated surface/ initial lung surface (1)

Secondly, the Vfads ratio that denotes the ratio of the final deformed contaminated surface at advanced lung cancerous stage divided by the initial lung surface.

Vfads = final deformed contaminated surface at advanced lung cancerous stage/ initial lung surface (2)

In fact, the FEM can provide calculation of surfaces for deformed and non deformed lung shape but if we consider a surface per unit thickness, we can transform this area ratio into volume ratio. So both ratios are being characteristic of a unit volume of the lung.

The FE simulation that we have presented in this study deals with different values of predefined internal pressure (Pi). The choice of the internal pressure spectrum which is varying in the range [10 to 40 kPa] was established based on experimental considerations involved in different references [13-17]. In fact, authors in reference [13], have studied the impact of pressure evolution in the thorax on the lung volume evolution for normal and pathologic cases and they have examine the interest of P-V curves based on experimental data. As far as we are interested with behavior of cancerous lungs, we have considered the following analysis.

The methodology of calculation applied at this step consists on determining the evolution of lung volume in two stages. The first stage is the study of the lung volume evolution with primary infected lung tissue versus pressure. To make an independent lung volume parameter that can be applied to different patients without considering their lung geometric shape, we have defined in this case curves corresponding to variation of Vfds parameter and pressure Pi (Pi = 10, 20, 30, 40 kPa). In a second stage, we have determined the changes i

volume of a cancerous lung within an advanced stage and the pressure Pi, so that we have outlined the Vfads parameter versus pressure Pi. We have then compared these two developments for different patients and we have established the following conclusions:

The evolution of the lung volume ratio is increasing almost linearly with pressure as it is shown by figure 17. Indeed, for different patients and for both configurations of a primary stage cancer and advanced one, the volume fraction increases when the pressure increases. This FE finding is in concordance with the experimental results due to reference [13].

We have attempted also to classify the volume fractions as a function of BMI associated to both configurations, primary lung cancer stage and advanced stage. We have found a decreasing trend of volume ratio as a function of BMI, (figure 18 and figure 19) this finding also meet results established experimentally in reference [13].

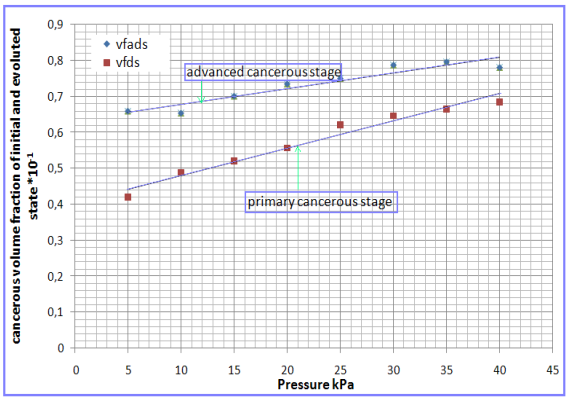

Fig 17 linear trends of both volume fractions (vfds and vfads) vs internal pressure for the first patient.

In patient's cases with primary cancer stage, we have noticed a faster evolution of pulmonary volume fraction against pulmonary pressure as it is shown by figure 17. In fact, the rate of volume fraction over pressure is higher in initial cancerous stage then in advanced case. This can be explained partially by the hyper sensitivity of lung tissue to endure internal pressure. Indeed, advanced cancerous stage is still marked by an invasion of infected lung tissue higher than an early stage cancerous lung. This fact may also be attributed to higher resistance to pressure evolution of the lung tissue and subsequently a lower convergence toward increasing the relative volume variation versus pressure increasing.

Table 3

Patient	Gender*	Vfds	Vfads	BMI
1	M	0,042	0,066	30
2	M	0,0929	0,097	28
3	M	0,06	0,065	29
4	M	0,054	0,08	30
5	M	0,08	0,1	24
6	W	0,03	0,04	30
7	W	0,02	0,03	35
8	W	0,014	0,016	40
9	W	0,0254	0,028	35
10	W	0,036	0,037	30

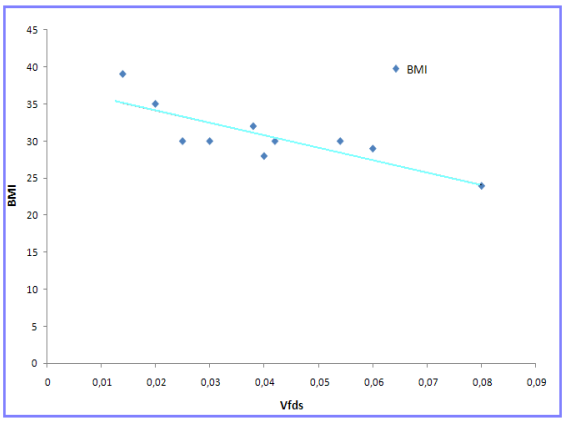

Fig 18 variation of the BMI vs the vfds the linear trend of this graph show that for patients with high BMI values, the volume fraction of the infected tissue is almost lower.

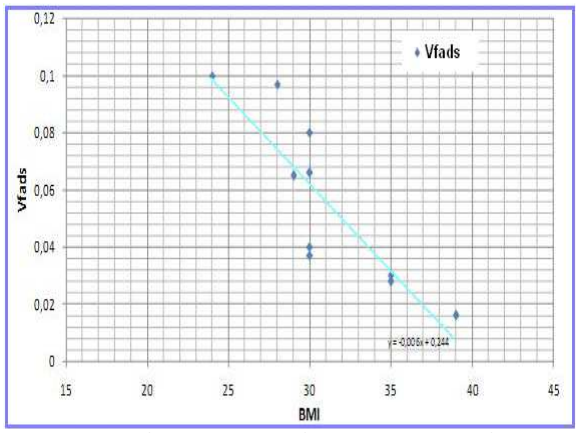

Fig 19 variation of the BMI vs the vfads the linear trend of this graph show that for patients with high BMI values, the volume fraction of the infected tissue is almost lower.

It is shown by Figure 18 and Figure 19 that the rate of the vfads over BMI is higer than the vfds rate over BMI. This fact is also done in other patients curves so that we can realize that the volume fraction of the primary cancerous stage tissue is less sensitive to BMI variation, and it accords a slow progression vs the BMI evolution. Conversally, the advanced cancerous stage of lung tissue is more sensitive to the BMI and we observe a rapid decrease in the volume fraction vfads when BMI factor increses.

5.2 Second FE parametric analyses

In another step we have addressed a second parametric numerical study that deals with new parameters which are describing the disease severity. By means of these new clues associated to numerical simulations, we will define the following parameters, and then study their evolution for the different patient's cases.

We have defined at first the following parameter; K_TL = stress intensity factor in the lung tissue affected by the tumor cells. K_TL measures the ratio of maximum stresses found in a field of lung tissue surrounding the infected tissue, divided by the average mean stress of lung tissue in the same region. Thus, the surface surrounding the infected tissue is defined so that the maximum thickness of this surface is equal to the maximum thickness of the infected tissue. We have represented the evolution

non dimensional parameter for patients listed in table 1, and then we have compared results of this parameter for initial cancerous stage and advanced stage. Table 4 resumes the different K_TL factors for patients listed by table1. as it is shown in this table the stress intensity factor K_TL for lung tissue is higher in the case of advanced cancerous lung stage then it is in initial cancerous stage. This fact is attributed to the high change in the lung shape within the existence of advanced tumor cells; so that local stresses will increase in some regions much more than in others. This phenomenon contributes in heighten of the factor K_TL associated to the advanced cancerous lung.

Table 4

Patient	Gender	Smax Initial cancerous stage	S mean	k_TL	Smax advanced cancerous stage	S mean	k_TL
1	M	52,53	44,350	1,184	62,400	45,900	1,359
2	M	81,5	47,011	1,734	104,500	53,030	1,971
3	M	94,24	79,026	1,193	114,500	65,393	1,751
4	M	198,7	61,405	3,236	204,600	44,173	4,632
5	M	78,21	54,530	1,434	130,300	61,856	2,107
6	W	117,3	62,518	1,876	156,540	50,308	3,112
7	W	106,3	48,261	2,203	208,600	63,556	3,282
8	W	26,07	25,369	1,028	39,110	34,399	1,137
9	W	140	57,649	2,429	203,800	65,070	3,132
10	W	155,8	47,651	3,270	219,100	64,577	3,393

Secondly, we have defined another ratio denoted by dvr; this ratio is an independent parameter that indicates the density of the geometric shape of the tumor tissue, but it takes into account the distribution of the tumor surface mass relative to total lung tissue surface mass defined in the same region. dvr= the surface of cancerous lung tissue divided by the entire lung surface.

At least we have denoted by r the ratio of the two parameters; K_TL and dvr; r= K_TL/dvr. Now we can address this new parameter to estimate the relative gradient of the stress intensity factor, because it allows inferring severity of concentrated stresses per unit of lung volume. Indeed, the value of this parameter indicates that the lung mass endure a large or a small change in stresses and strains in the presence of tumor tissue in the lung tissue.

Outstandingly since this factor is as more significant as the severity of the disease is important, because for a low volume of lung tissue there is a large gap of constraints in this tissue. Thus, the risk of acute respiratory disorder is significant. We tried to calculate this factor from different patients listed by Table 1. Results of these calculations are considered in Table 5 below.

Table 5

Patient	kt1*	r1= kt1/dvr	kt2*	r2=kt2/dvr	BMI
1	1,184	28,201	1,359	40,570	30
2	1,734	18,650	1,971	28,151	28
3	1,193	19,875	1,751	35,019	29
4	3,236	57,924	4,632	59,897	30
5	1,434	17,928	2,107	21,065	24
6	1,876	62,542	3,112	77,791	30
7	2,203	109,131	3,282	110,405	35
8	1,028	73,402	1,137	113,695	40
9	2,429	95,550	3,132	110,356	35
10	3,270	90,450	3,393	90,560	30

As r ratio is independent from the geometry, it is characteristics of pure lung tissues properties. Consequently, it is found out that in females the rate r= K_TL / dvr is a bit higher than in male's patients for similar dvr ratios, Figure 20.

We also note that there is some dependence of the r factor with the BMI; in fact, according to table 5, we can conclude that obesity promotes the severity of the stresses in the vicinity of the tumour tissue which increases the r factor for these patients. Thus, obese patients are more susceptible to lung problems when lung tumour is present.

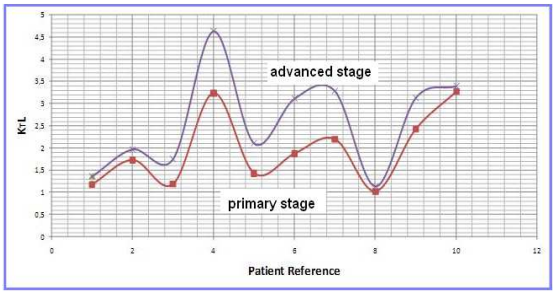

Fig 20 Stress intencity factor ktL for two cancerous stages with different patients.

6. Conclusions

This paper has presented an innovative methodology for efficiently analysing and exploring critical lung disease such as pulmonary cancer. We have presented the methodology used to detect crucial mechanical properties according to geometric parameters deduced from medical CT images. Basically, the FE technique combined to image data processing has lead to establish the difference between mechanical parameters in various pathologic lungs. Mechanical parameters were used to enhance the comprehension and the analysis of lung cancerous diseases of various patients.

The identification of tumour lung tissues in CT images is not easy to be precisely defined and consistent with reality. It requires a large experience and high competence. To meet this need, a suitable mathematical approach has been used to detect the contaminated cancerous lung tissues. This step was very important before a transition for building FE models based on the organs shape captured via 2D CT images. In fact, the FE modelling was possible through combination of various techniques based on Matlab capabilities, CATIA software and Abaqus commercial code.

The 2D finite element CT based modeling is established to investigate essentially stresses at various pressures. In this analysis, the von Mises effective stress, pressure distribution and maximum principal stresses in the overall organs as well as pathologic mechanics were investigated. The computed stress behavior of the different tissues is qualitatively consistent with the experimental results established in the literature for the spectrum of pressures used in this study.

The parametric FE study has enabled investigation of distribution and magnitude of various lung tissue parameters under pressure. We can establish that such a method has provided a useful complement to experimental and analytical models. Thus, this technique was u substantiate mechanical and material parameters

various lung tissues and the, and then enhance the behavior of lung tissues in the lung cancer pathology. This fact has reveals the effect of mass distribution of cancerous lung tissues. Thus, it has been established that increase of BMI factor can promotes stress concentration at the vicinity of tumor lung tissue. We have introduced some mechanical parameters to describe the behavior of lung tissue and to find correlation between geometric parameters of tumor lung tissue and mechanical parameters.

The methodology used in this study can support understanding physiological and clinical relevant lung problems, while analyzing the evolution of lung damage caused by carcinoma cells.

In addition to cancers diseases, the procedure of analysis and simulation described in this article can also be used for a variety of respiratory diseases and distress syndromes. Indeed, it can be used by the clinician for several purposes. It should enable clinicians, based on prior health data of a patient (CT scanned image) to provide the response of the entire rib cage and the different organs before surgery, especially for forced ventilation when the respiratory function of a lung are exhausted. It can allow adapting and even customizing ventilation parameters according to each patient's respiratory mechanism and thus protect the patient lung from damage, in the case of forced respiration. The methodology described here can allow also the different stages of diseases, and making right predictions. It can be performed to determine the appropriate conditions before injury and can also provide the basis for quantitative analysis and the integration of information into the radiotherapy scheduling, treatment, and follow-up process.

References

[1] Barry J. Doyle, Aidan J. Cloonan, Michael T. Walsh,David A. Vorp, Timothy M. McGloughlinJ, "Identification of rupture locations in patient-specific abdominal aortic aneurysms using experimental and computational techniques", J. Biomechanics. 43 (2010) 1408–1416.

[2] Jae-Hoon Chung, Vijay Rajagopal, Tod A. Laursen, Poul M.F. Nielsen, Martyn P. Nash, "Frictional contact mechanics methods for soft materials: Application to tracking breast cancers", J. Biomechanics. 41 (2008) 69–77.

[3] Chun Xu, Michael J. Brennick, Lawrence Dougherty, David M. Wootton, "Modeling upper airway collapse by a finite element model with regional tissue properties", J. Medical Engineering & Physics. 31 (2009) 1343–1348.

[4] Saleh Alsubari1, Hassan Chaffoui, "Comparison of the elastic coefficients and Calculation Models of the Mechanical Behavior one- Dimensional Composites", IJCSI International Journal of Computer Science Issues, Vol. 8, Issue 5, No 2, (2011) 63-67

[5] P. Sushil Kumar, M. Shorif Uddin, S. Bouakaz., "Extraction of Facial Feature Points Using Cumulative Histogram", IJCSI International Journal of Computer Science Issues Vol. 9, Is(3) (2012) 44-56.

[6] Mark A. Baldwin, Joseph E. Langenderfer, Paul J. Rullkoetter, Peter J. Laz, "Development of subject-specific and statistical shape models of the knee using an efficient segmentation and mesh-morphing approach", computer methods and programs in biomedicine. 97(2010) 232–240.

[7] Alexandre Hostettler, Daniel George, Yves Rémond, Stéphane André Nicolau, Luc Soler, Jacques Marescaux, "Bulk modulus and volume variation measurement of the liver and the kidneys in vivo using abdominal kinetics during free breathing", Computer methods and programs in biomedicine. 100 (2010) 149–157.

[8] Cynthia L. Eccles, Laura A Dawson, Joanne L. Moseley, Kristy K. Brock, "Inter fraction liver shape variability and impact on GTV position during liver stereotactic radiotherapy using abdominal compression", Int. J. Radiation Oncology Biol. Phys. 80 (2010) 938–946.

[9] Stephen J. Lai-Fook, Kenneth C. Beck, Alison M. Sutcliffe, Jonathan T. Donaldson, "Effect of edema and height on bronchial diameter and shape in excised dog lung, Respiration Physiology". 55 (1984) 223–237.

[10] V. Caselles, R. Kimmel, G. Sapiro, "Geodesic active contours", International Journal of Computer Vision. 22 (1997) 61–79.

[11] Nock, Richard and Nielsen, Frank, "Statistical Region Merging", IEEE Trans. Pattern Anal. Mach. Intell. 26 (2004) 1452–1458.

[12] Matt Dunbar, ABAQUS/Explicit manuel, version 6.7, Dassault Systèmes, Providence, 2007.

[13] R Scott Harris MD, "Pressure volume curves of the respiratory system", Am. J. Respir. Crit. Care Med. 50 (2005) 79–99.

[14] VM. Ranieri, R. Giuliani, T. Fiore, M. Dambrosio and J. Milic-Emili, "Volume-pressure curve of the respiratory system predicts effects of PEEP in ARDS": "occlusionversus "constant flow" technique, Am. J. Respir. Crit. Care Med. 149 (1994) 19–27.

[15] RS. Harris, DR. Hess, JG. Venegas, "An objective analysis of the pressure-volume curve in the acute respiratory distress syndrome", Am J Respir Crit Care Med. 161 (2000) 432–439.

[16] T. Mutoh, WJ. Lamm, LJ. Embree, J. Hildebrandt, RK. Albert, "Abdominal distension alters regional pleural pressures and chest wall mechanics in pigs in vivo", J. Appl Physiol. 70 (1991) 2611–2618.

[17] David Richens, Mark Field, Shahrul Hashim, Michael Neale, Charles Oakley, "A finite element model of blunt traumatic aortic rupture", European Journal of Cardio-thoracic Surgery. 25 (2004) 1039–1047.

Fatma Ayari: is Graduate Research Assistant of Electrical engineering. She is a PhD student in Electrical Engineering at the National School of Engineering, Tunisia. She teaches undergraduate courses in Programming Mathematics and Informatics. She's research areas of interest include experimental and computational signal processing, neural networks and automatics. She has published in journals and proceeding conferences as IEEE proceedings.

Mekki Ksouri: is Professor in the of the Department of Electrical and Computer Engineering automatics and Electrical engineering at the National School of Engineers of Tunis Tunisia. His research interests include distributed computing, neural networks, fuzzy systems, genetic and ellipsoid algorithms bioinformatics and biomimetic and bio-Inspired Computing Machines, author of scientific books. He has published a great number of scientific papers published in various IEEE and other international journals. His recent research has been supported by many international organizations, INRIA, AUF.

Ali Alouani: Professor in the Department of Electrical and Computer Engineering Tennessee Technological University. He developed and taught many undergraduate and graduate courses in the Systems and Signals areas. Till date he has published in more than 120 technical journal and conference papers. He holds 4 patents.

Nomenclature

S_{min}: Von Mises minimum stress
S_{max} : Von Mises maximum stress
V_{fds} : volume fraction of deformed shape
V_{fads}: volume fraction of advanced deformed shape
P: pressure
K_TL: stress intensity factor in the lung tissue
d_{vr}: surface of cancerous lung tissue divided by the entire lung surface.
r: K_TL/d_{vr}